Experimental Study on the Performance of Small-Scale Wind Turbine Rotors

Gabriela Cîrciumaru, Rareș-Andrei Chihaia, Dragoș Ovezea, Ionel Chiriță, Sergiu Nicolaie, Lucia-Andreea El-Leathey and Adrian Nedelcu

INCDIE ICPE-CA
Bucharest, Romania
gabriela.circiumaru@icpe-ca.ro, rares.chihaia@icpe-ca.ro, dragos.ovezea@icpe-ca.ro, ionel.chirita@icpe-ca.ro, sergiu.nicolaie@icpe-ca.ro, andreea.elleathey@icpe-ca.ro, adrian.nedelcu@icpe-ca.ro

***Abstract*—The paper presents the results of the research regarding the development and testing of small-scale wind turbine rotors, as well as aspects regarding their integration in power systems. Different wind rotors with diameters ranging from 524 mm to 620 mm have been designed in order to study the influence of the main parameters such as rotor diameter, blade chord length and pitch angle on the power output. The models have been made by 3D printing and were characterized by testing performed in an open circuit wind tunnel. For 10 m/s wind velocity, the maximum power output of the developed rotors is in the range of 34…48 W. The experimental results revealed that the lower the pitch angle, the higher the starting velocity, turbine power, rotational speed and power coefficient.**

***Keywords*—wind rotor, wind tunnel testing, power curve, power coefficient, blade**

I. Introduction

The use of renewable energy sources, especially wind energy, has been steadily rising over the last decade, as a result of the increase in the global energy demand and of the environmental targets. Starting with 2014, more than 50 GW of new wind energy has been installed every year [1]. As a result, the energy markets are in a continuous transition and governments "focus on how to improve the integration of renewables and to capture the most value" [1]. The industry, as well, has to reinvent itself.

With the significant growth of the wind energy sector, an increase in studies and research to improve the performance of existing turbines or to develop new types of wind energy conversion systems has been also registered. The blade element model is investigated to extend its application to the turbulent wake regime for horizontal axis wind turbines [2] or for optimizing a counter-rotating wind turbine (CRWT) by predicting the front rotor flow and the wake generated by it [3]. A new experimental model of 1 kW CRWT is investigated in [4]. The tests showed an average power increase of 60% brought by the use of the second rotor for 10 m/s wind velocity. Other research focus either on assessing the performance of wind farms by comparing the use of CRWT systems [5] in different configurations with one rotor turbines or on comparing the power produced by single rotor turbines with dual rotor turbines [6].

The paper aims to present the results of the research regarding the development and testing of small-scale wind turbines rotors, as well as aspects regarding their integration in power systems. Thus, the researchers from the Renewable Energy Sources Laboratory of ICPE-CA conducted a research project [7] envisaging an increase in the energy efficiency of wind power conversion systems. There have been designed, developed and characterized in a wind tunnel small scale wind rotors (experimental models) with different diameters. The blades have increased chord length, allowing the start of the rotor at lower wind speeds; thus, the turbines can be used in different applications, involving low power demand (households, rooftops, urban landscape etc.) or innovative systems (counter-rotating wind turbine systems).

II. Development of Small-Scale Wind Turbine Rotors

In order to develop the experimental wind turbine models, the following steps were envisaged: designing of different sizes of wind rotor blades, 3D printing of the models, testing performed in open circuit aerodynamic tunnel, analysing the experimental results.

A. Design of the wind turbine rotors

Given the constraints of the open circuit wind tunnel, rotors should not exceed a certain size, namely 2/3 of the test chamber size of 1 m. Taking into account the rotors size (maximum 660 mm), the Betz limit and the wind velocities at which the testing would be performed, the power output expected should be in the range 20...45 W.

Different sizes of rotors were designed and made in order to study the influence of the main parameters such as rotor diameter, blade chord length and pitch angle on the power output. This will also provide a subsequent integration in counter-rotating systems. Thus, to minimize the wind tunnel effects it was decided to design and realize the biggest rotor with a maximum diameter of 620 mm (out of which 100 mm is the rotor hub). The other two rotors vary in size as follows: 586 mm and 524 mm respectively. In order to design the rotors, several NACA aerodynamic profiles were analysed using the open access QBlade software: 4406, 4412 (see Figure 1), 4424, 9412 and 9912. In the first step of the analysis, a 260 mm blade profile with a chord (c) of 40 mm was considered. For each of the above-mentioned NACA profiles, the maximum power coefficient C_p and the pitch angle were determined.

$$C_p = 2P/\rho A V_{wind}^3 \quad (1)$$

where P is the theoretical power of the wind turbine, ρ is the air density, ρ =1.205 kg/m^3 at 20°C, A is the area swept by the blades at one spin of the rotor, $A=\pi R^2$ with R the wind rotor radius and V_{wind} is the wind velocity.

Conclusions resulting from this analysis led to the selection for further performance analysis of NACA 4412 profile.

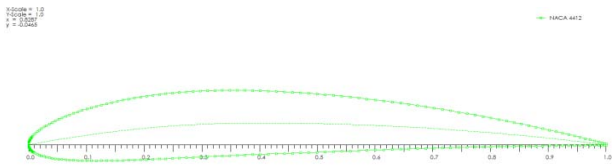

Fig. 1. NACA 4412 aerodynamic profile obtained using QBlade

The optimization of the blade for different tip-speed ratios

$$\lambda = V_{tip}/V_{wind} \quad (2)$$

where V_{tip} is the linear velocity at blade's tip, showed that for high values of λ (e.g. λ=7) the chord decreases significantly (see Figure 2) and so does the lift. In order to obtain the required power, in the second stage of the analysis, the solidity has been increased and the blade was optimized for $\lambda = 3$. Thus, in accordance with [8], [9] specifying that for $\lambda \leq 3$ the solidity, σ, increases, a double chord of 80 mm (see Figure 2) was considered for these profiles.

$$\sigma = A_b/A \quad (3)$$

A_b represents the area of the blades.

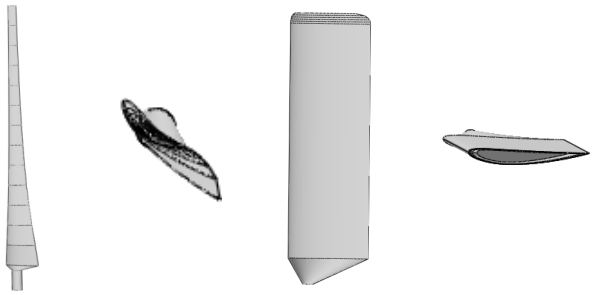

Fig. 2. NACA 4412 aerodynamic profile: left c=40 mm and λ=7; right c=80 mm and λ=3

Thus, there have been designed 3 pairs of blades with the geometrical characteristics given in Table I; *x* represents the position and *c* the chord of the blade.

TABLE I. GEOMETRICAL PARAMETERS OF THE NACA 4412 BLADES

Rotor 620 mm, blade 260 mm		**Rotor 586 mm, blade 243 mm**		**Rotor 524 mm, blade 212 mm**	
x [mm]	***c [mm]***	***x [mm]***	***c [mm]***	***x [mm]***	***c [mm]***
0	10	0	10	0	10
25	80	22.23	75	17.21	66
250	80	233.38	75	203.27	66
252	79.6	235.26	74.7	204.92	65.82
254	78.33	237.14	73.51	206.57	64.77
256	76	239.02	71.32	208.23	62.84
258	72	240.89	67.57	209.88	59.54
260	60	242.77	56.31	211.54	49.61

B. *Development of wind turbine rotors*

The blades and the hub of the experimental models of wind turbines rotors were made of ABS by 3D printing, using a Fortus 360 mc large printer. In order to streamline the printing process while maintaining the mechanical strength, it was chosen for the blades to have a solid outer layer, with a thickness of 1.2-1.5 mm (made of 4 layers) and a square structure woven inside (see Figure 3). This led to a reduction in printing time and reduced material consumption. In order to increase the strength of the blades, at a distance of approximately 30% of their length, galvanized metal rods were introduced, as follows: for two front blades, a Ø4 mm rod, and for one front blade and the rear blade, respectively, one Ø6 mm rod.

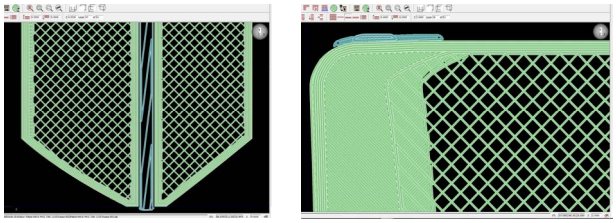

Fig. 3. Details on the internal structure of the blades – stiffening rod area (left) and full outer layer area (right)

After printing the blades, the backing material was removed by dissolving in a sodium hydroxide liquid bath. To reduce the possible influences on the blades aerodynamics, their surface was processed (by sanding or painting with rubber paint) so as to be as smooth as possible.

III. TESTING OF THE SMALL-SCALE WIND TURBINE ROTORS

The test rig used for wind turbine rotors characterization consists of an open circuit wind tunnel (see Figure 4) equipped with different measurement and control equipment. The tunnel allows the testing of rotors from velocities of 2 m/s up to 30 m/s. The wind tunnel is provided with a test section of 1x1 m and a visualisation window of 0.6x1 m. The maximum deviation from flow uniformity in the test section is: ± 0.2 m/s for velocities in the range 2÷5 m/s, ± 0,3 m/s for velocities in the range 5.1÷10 m/s and ± 3%·v_p, respectively, where v_p represents the pre-set velocity.

Fig. 4. Open circuit wind tunnel

The velocity range is provided by a fan of 22 kW, 3x380 Vca, 50 Hz, and 975 rpm, controlled by a frequency converter AVD200 type. In the proximity of the test section are located the control panels of the fan, mechanical loading system and parameters measuring devices.

In order to determine the characteristic power and torque curves of the small-scale models, the rotors were mounted in the centre of the test chamber, on the adjustable height support tower, which embeds the torque, speed and force transducers. All measuring and control equipment was connected and, by changing the fan speed, the rotors were tested to different wind velocities, in the range [9÷12] m/s. Using the mechanical loading system (Mobac FRAT 50

brake), different torque values were provided for each rotor, allowing power curve plotting for different velocities.

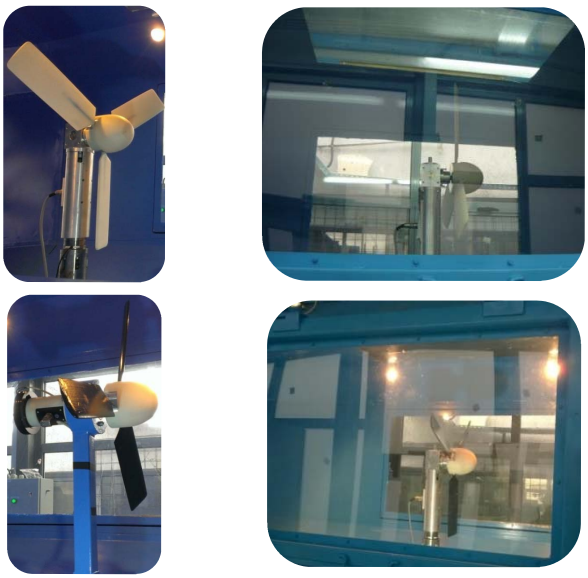

Fig. 5. Testing of the wind rotors in the open circuit wind tunnel

Both instantaneous and mediated measured values (time, air velocity, rotational speed, forces and torques on the 3 axes) were displayed and recorded. The values were separately analysed for each rotor and the characteristic power and torque curves were plotted as a function of rotational speed $P = f(n)$, and $T = f(n)$, respectively. For the determination of the power the following equations were used:

$$P = \omega T \quad (4)$$

with the angular speed

$$\omega = 2\pi n/60 \quad (5)$$

IV. Results and Discussions

The characteristic curves $P = f(n)$ and $T = f(n)$ for wind velocities between 9 and 12 m/s are shown in Figures 6 and 7 for the 620 mm diameter rotor. Comparative graphs presenting the power and torque versus rotational speed at 10 m/s air velocity are shown in Figures 8 and 9. The results of the testing showed that the power output of the developed wind rotors at 10 m/s air velocity is as follows: 22 ÷ 48 W for the 620 mm diameter rotor, 27 ÷ 37 W for the 586 mm rotor and 27 ÷ 34 W for the 524 mm rotor.

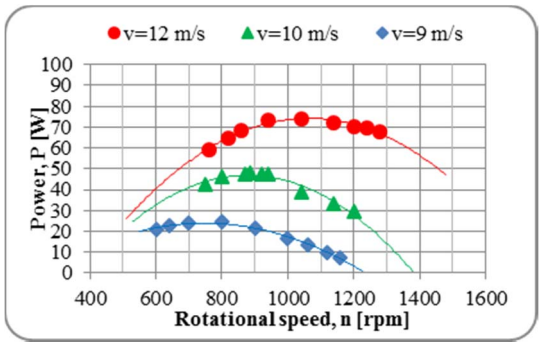

Fig. 6. Characteristic power curves for the 620 mm diameter rotor

The influence of the pitch angle on the power coefficient was also investigated. Figure 10 presents the results for the 524 mm diameter rotor.

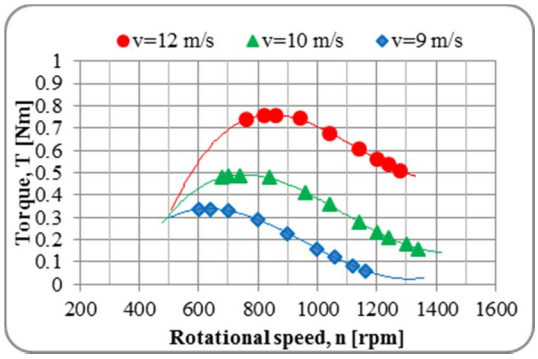

Fig. 7. Characteristic torque curves for the 620 mm diameter rotor

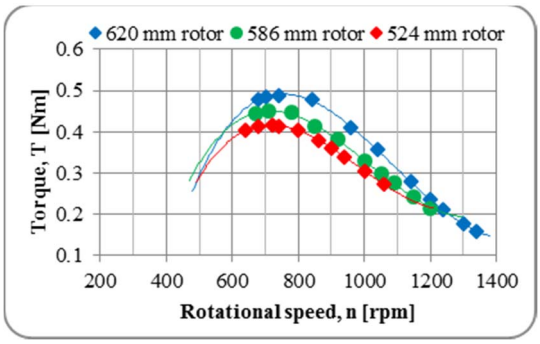

Fig. 8. Characteristic torque curves of the rotors at 10 m/s wind velocity

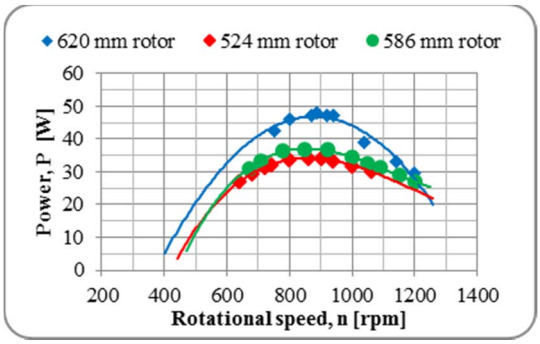

Fig. 9. Characteristic power curves for the selected rotors at 10 m/s wind velocity

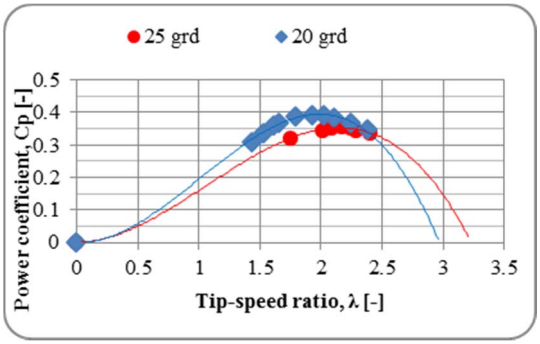

Fig. 10. Power coefficient versus tip-speed ratio for the 524 mm rotor at 10 m/s wind velocity

The tests revealed the following: the lower the pitch angle, the higher the starting velocity, turbine power, rotational speed and power coefficient. Thus, a good C_p is obtained but it comes with some shortages like increased

starting velocity. For ensuring the highest power output, a compromise between the pitch angle and the other relevant parameters mentioned above has to be made, depending on each application operating conditions.

V. Small scale wind turbine integration in power systems

Recently, renewable energy and distributed generation systems (DGSs) have attracted increasing attention and have been extensively researched due to their many advantages. The current improved versions of DGS make them applicable to a grid-tied system or an isolated system suitable for converting wind power, solar energy, hydropower, etc. Large scale wind farms can be easily integrated into the grid using dedicated power stations which ensure the control and power transfer of wind turbines. On the other hand, the small scale wind turbines are not a convenient option for locations with grid access due to their operation intermittence and unpredictability. This is why the microgrid concept comes in handy because it can integrate multiple DGSs to ensure the continuous operation with or without connection to a wide area synchronous grid. Just by joining together wind turbines with PV panels and storage capacities, the operation of a microgrid system is greatly enhanced. There are still some challenges approached by research conducted worldwide.

Emerging power electronic technologies and digital control systems make possible to build advanced microgrids capable to operate independently from the grid and integrating multiple distributed energy resources. There are a lot of challenges in integration, control, and operation of microgrid to whole distribution system. Microgrid is not designed to handle the large power being fed by the utility distribution feeders [10]. Moreover, due to the intermittence of renewable energy and DGS, bidirectional dc/dc and dc/ac converters are usually required to feed the connected loads with smooth power [11]. There are two modes in which microgrid operate: the grid connected mode and the stand-alone mode or islanded mode. In grid interfaced operation mode, point of common coupling (PCC) is closed and microgrid is linked with utility grid. Whenever there is any disturbance in utility grid or microgrid, PCC is opened and the microgrid is disconnected to the main grid, then it is operated in stand-alone mode [12].

Small wind turbines can be defined as turbines that are specially designed for built environment, and can be located on buildings or on the ground next to buildings (different environment compared to wind farms). This implies that the turbine has to be adapted for the wind regime in the built environment and can resist wind gusts and turbulences. Furthermore, the shape and size of the turbine has to be designed to visually integrate with the surrounding buildings. These small wind turbines can also be referred to as “urban wind turbines“ [13]. If there is a surplus of electricity generated from a small wind turbine, it can be fed to the grid and sold through a billing scheme agreed with the electricity supply company based on a prosumer contract.

The aim of the future research in this field is focused towards finding the main influential factors in determining the maximum allowable level of wind energy integrated in microgrids. Especially with growing trend of wind energy integration in distribution systems, dynamic issue such as fault and post-fault recovery condition of wind integrated systems cannot be neglected together with static issues while determining the suitable penetration level of wind energy in microgrid system [14].

VI. Conclusions

The paper presents the development of small-scale wind rotors designed for obtaining a power of 20...45 W at 10 m/s air velocity. The models have NACA 4412 untwisted blades, with a maximum chord length of 80 mm and are made of ABS, by 3D printing. Their testing in an open circuit wind tunnel at different wind velocities led to obtain the following maximum power output at 10 m/s wind velocity: 48 W at around 900 rpm for the 620 mm diameter rotor, 37 W at around 850 rpm for the 586 mm rotor and 34 W at approximately 860 rpm for the 524 mm rotor. Thus, the performed tests have confirmed a minimum of 20 W power output for 10 m/s wind velocity, supplied by the developed rotors. The future development of the research envisages their integration in counter-rotating wind turbine systems in order to investigate their mutual influence and the energy contribution of the second wind rotor.

Acknowledgment

This work was financially supported by the following grants: NUCLEU no. PN 16 11 01 01, 14N/2016, project PN-III-P1-1.2-PCCDI-2017-0391/CIA_CLIM - Smart buildings adaptable to the climate change effects, within PNCDI III programme and project no. 30PFE/2018.

References

[1] Global Wind Energy Council, “Global wind report 2018”, April 2019, www.gwec.net

[2] S. Liu and I. Janajreh, “Development and application of an improved blade element momentum method model on horizontal axis wind turbines”, in Int. J. of En. and Environmental Eng. 2012, 3: 30.

[3] B. Hwang, S. Lee and S. Lee, “Optimization of a counter-rotating wind turbine using the blade element and momentum theory”, in J. of Ren. and Sust. En., 5, 2013, pg. 052013-1–052013-10.

[4] L.A. Mituleț, et al., “Wind tunnel testing for a new experimental model of counter-rotating wind turbine”, in Procedia Engineering, vol. 100, 2015, pg. 1141-1149.

[5] A. Vasel-Be-Hagh and C.L. Archer, “Wind farms with counter-rotating wind turbines”, Sustainable Energy Technologies and Assesment, 24(2017), pp. 19-30.

[6] V. Mishra and H.K. Paliwal, “Experimented examination of power produced for dual rotor wind turbine over single rotor wind turbine”, IJITEE, ISSN 2278-3075, vol. 9, iss. 2, 2019, pp. 2306-2311.

[7] Contract No. 14N/2016, “Innovative constructive solutions for wind turbines to increase their energy efficiency by small-scale modelling”.

[8] P.J. Schubel and R.J. Crossley,”Wind turbine blade design”, Energies, 2012, 5, pp. 3425-3449; doi:10.3390/en5093425.

[9] G. Ingram,”Wind Turbine Blade Analysis using the Blade Element Momentum Method”, Version 1.1, October 18, 2011, Durham Univ.

[10] T. Mulualem, Y. Khan, B. Khan (November 5th 2018). “Microgrid Integration”, Special Topics in Renewable Energy Systems, E. Yüksel, A. Gök and M. Eyvaz, Eds., IntechOpen, DOI: 10.5772/intechopen.78634;

[11] C. Abbey and G. Joos, “Supercapacitor energy storage for wind energy applications,” IEEE Trans. Ind. Appl., vol. 43, no. 3, pp. 769–776, May 2007.

[12] P. Singh and B. Khan, “Smart microgrid energy management using a novel artificial shark optimization”, Complexity. Vol. 2017, Article ID 2158926: 22p, https://doi.org/10.1155/2017/2158926.

[13] http://www.urban-wind.org/pdf/SMALL_WIND_TURBINES_GUIDE_final.pdf

[14] T. Aziz et al., “Integration of wind energy system in microgrid considering static and dynamic issues”, 2015 Int. Conf. on El. Eng. and Information Communication Technology *(ICEEICT)*, Dhaka, 2015, pp. 1-5, doi: 10.1109/ICEEICT.2015.7307479.